

Energy-Efficient Strain Gauges for the Wireless Condition Monitoring Systems in Mechanical Engineering

M. BERNDT, T. FELLNER, R. ZEISER and J. WILDE

ABSTRACT

This work focuses on the development of novel strain gauges, which are suited for the operation in autonomous wireless condition monitoring systems. For this purpose, capacitive as well as highly resistive strain gauges were designed and fabricated. The C- and R-sensors were utilised in combination with demonstration circuits, which integrate the circuits for instrumentation, A/D-conversion and furthermore comprise a microcontroller with a wireless transceiver system, all on a small separate printed wiring board. The authors will also be able to present a small demonstration system in operation during the oral presentation.

INTRODUCTION

Particularly, in the area of oversized machines (e.g. wind power plant, Figure 1), the use of wireless monitoring systems is becoming increasingly important [1]. These systems are used for monitoring the conditions of machine elements. They must be appropriate to collect, store and transmit data about the state of moving machine parts. An important parameter for the operation company and also for the manufacturer is the state of stress in the machine elements. Based on the



Figure 1. Wind power plant.

Michael Berndt, Thomas Fellner, Roderich Zeiser, Jürgen Wilde
University of Freiburg
Department for Microsystems Engineering (IMTEK)
Georges-Koehler-Allee 103
79110 Freiburg
Germany

experimentally observed deformation on a specimen a statement about the state of stress can be made. The known material properties in combination with the actual stress make a forecast possible of the construction failure. For this purpose, usually wired electric low resistive strain gauges are used, which due to their low resistance and high power consumption are not well-suited for wireless application. An interesting alternative to resistive strain gauges are sensors working on the capacitive principle. Another way to reduce the power consumption is to increase the resistance in the strain gauges.

DEVELOPMENT OF THE CAPACITIVE STRAIN GAUGES

Design

In the past, different concepts were presented to measure strain capacitive [2] [3]. Inter-digital electrodes in one plane on a flexible substrate are chosen as sensing principle for the strain gauge. The advantages of this principle are maximal transfer of strain into the capacitor, high capacitance in small place and only one process step for the electrodes in one plane.

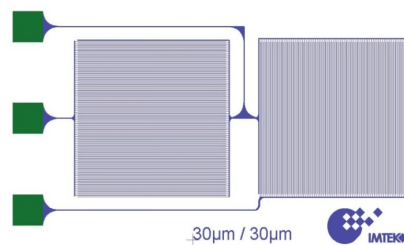


Figure 2. Sensor design as a measuring half-bridge.

Figure 2 shows the draft of a half-bridge also in one level perpendicularly to each other aligned sensors. In this case the structure width and distance are equal with a value of $30\ \mu\text{m}$. On the right side there are three soldering pads, where the capacitances can be connected for measuring. The ground electrodes are connected together and share a soldering pad. Sharp edges in the design are rounded to reduce the stress in these areas. For the analytic computation of an inter-digital capacitor different approaches can be found in the literature [4].

Simulation

A finite-element-simulation software (ANSYS) was used for the numerical calculation of the sensor sensitivity. The chosen multi-physics simulation combined the results of a mechanical analysis with an electrostatic analysis. In the mechanical part of the simulation strain is applied to a specimen with the properties of steel. The strain is transferred through an adhesive film into the sensor substrate and creates a displacement of the electrodes. This displacement leads to a change of the capacitance compared to the state without strain. By iterative simulations it is possible to optimise the geometric and material dependent parameters of the strain gauge with regard to high sensitivity. Established on the computation, several main design rules for the sensor could be made. The sensor substrate should not be thicker than the pitch of the

electrodes. The sensitivity correlates directly with the substrate thickness. The gauge factor increases with decreasing distance of the electrodes. The thinner the metallization of the electrodes is, the more linear is the dependence on the strain of the capacitance.

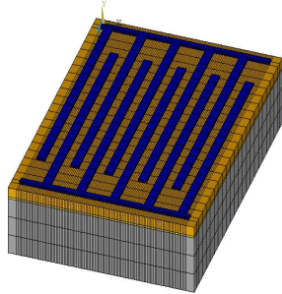


Figure 3. Meshed geometry of the sensor electrodes.

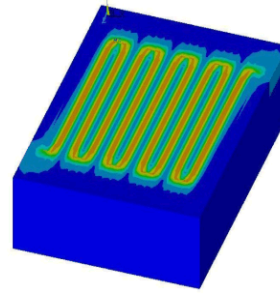


Figure 4. Electrostatic simulation of the strain gauge.

The ratio of width and distance was optimised for a higher capacitance. An increase of the sensitivity for 45 μm width and 15 μm distance was obtained as a result of simulation (Figure 3 and 4). The change of capacitance over strain is linear with a strain sensitivity of -0.57 pF/%. This corresponds to a gauge factor of -1.23. With this simulation, it is possible to predict the value of the sensor capacitance before the fabrication. The simulated value corresponds to the measured value after the fabrication with a divergence of 4%.

Manufacturing

The first material used as a substrate for the strain gauge is polyimide. It is a standard material for resistive strain gauges with outstanding properties like high thermal and chemical stability. A disadvantage of polyimide is its high absorption of humidity which is about 3 % [5]. For that reason, a second substrate was utilised, LCP – Liquid Cristal Polymer. This material, recently available as a foil, is mostly known as a material for premolded packages. The value of humidity absorption is about 0.03 % [6], and a hundred times smaller than for polyimide. To process both polymer foils, with approved thin film technologies, the foils are temporarily bonded on carrier substrates with an adhesive that is residue-free removable after the processing. For the reproducibility in widths and distances for the designed electrodes it is necessary to use photolithography for the processing. In this work a lift-off process is chosen for the patterning of the structures because of its outstanding accuracy.

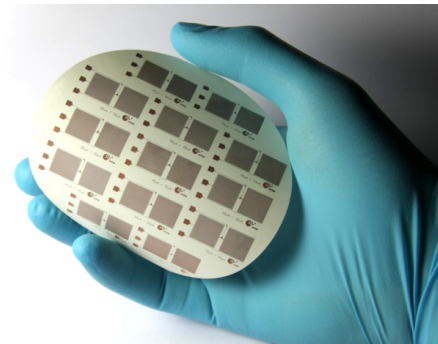
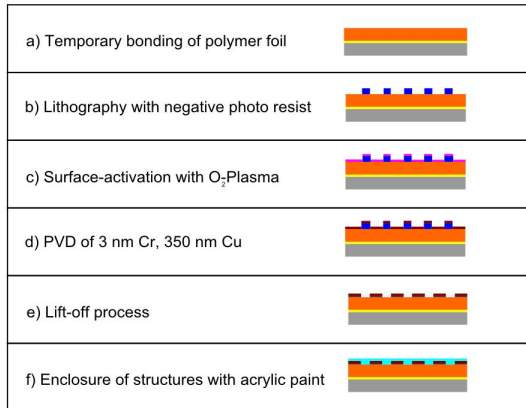


Figure 5. Process flow for the capacitive strain gauges. Figure 6. Sensor structures on LCP substrate.

Figure 5 shows a cross section of the sensor electrodes and describes the different fabrication steps. Step a) is the temporary bonding of a 50 μm polymer foil on a standard silicon-wafer, used as carrier substrate. In b) a negative photoresist is spin coated on the polymer foil and structured by photolithography. To clean the surface, an O₂-Plasma is ignited in c). In d) 3 nm and 350 nm metallisation of Cr and Cu are deposited by evaporation. In step e) the electrodes are patterned by the lift-off process of the sacrificial photoresist and the metallization on it. In f) the sensor structures are encapsulated with an acrylic varnish for protection against humidity and particles. After the fabrication process the polymer foil is detached from the carrier substrate and diced. Figure 6 show the sensor structures on the substrates LCP before dicing.

Characterisation

For the characterisation of the sensors different environmental conditions are necessary. Particularly temperature and humidity influences are expected. As a test specimen for the strain gauges a spring steel ribbon, with an ultimate elongation of one percent, was selected. For the characterisation, the sensor prototypes are mounted with an acrylic adhesive on the steel ribbon (Figure 7). The tensile testing set up is integrated into a heat chamber. So it is possible to measure the influence of temperature on the sensor signal. To measure the influence of humidity, generated water vapor was led into the heating chamber (Figure 8). Pure nitrogen is used to create an atmosphere of 0% relative humidity. Several temperature and humidity sensors inside ensure the adjustability of the chamber.

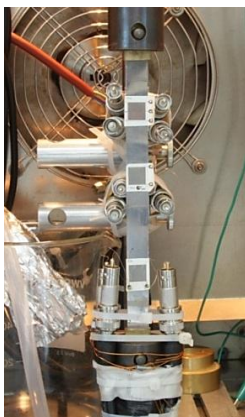


Figure 7. Tensile testing.



Figure 8. Setup with heating chamber.

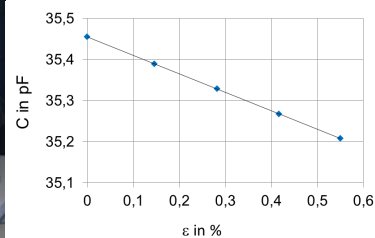


Figure 9. Capacitance as a function of strain.

In Figure 9 the results of a strain measurement with a sensor on polyimide with an electrode width of 45 μm and a distance of 15 μm are presented. The measurement took place at a room temperature of 23 $^{\circ}\text{C}$ and 0% relative humidity. The slope of the regression line for the measured values corresponds to the strain sensitivity and is -0.658 pF/%. Normalised to the absolute capacitance $C_0=47.74$ pF, the strain coefficient is $SC=13,783$ ppm/%. This corresponds to a gauge factor of -1.38. The output characteristic of the capacitive strain gauge is linear. The same experimental setup allowed obtaining the capacitance of the prototype sensors at different temperatures and different humidities. The sensor capacitance shows a linear dependency on humidity and temperature. The obtained coefficients for the sensitivities are $HC = 1435$ ppm/%rH and $TC = 2168$ ppm/K. The same investigation was realised for the capacitive strain gauges made of LCP.

DEVELOPMENT OF THE HIGH-OHMIC RESISTIVE STRAIN GAUGES

Design

The cross-axis sensitivity of the high-ohmic resistive strain gauges concept is only depending of the temperature. The compensation of the temperature dependence can be managed over the arrangement by bridge connection. Four strain gauges were integrated as full-bridges to compensate the cross-sensitivities of the sensor. Furthermore the temperature coefficient is adjustable over the alloy composition NiCr (Figure 10).

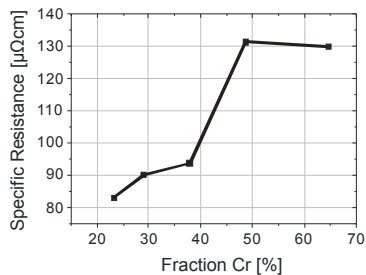


Figure 10. Influence of Cr-Fraction on Resistance.

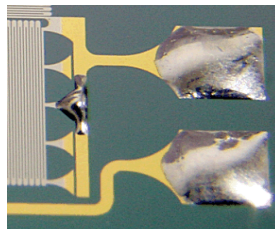


Figure 11. Trim structure from resistive strain gauges.

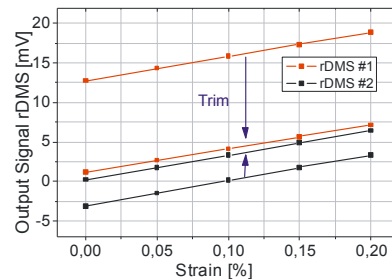


Figure 12. Offset correction through trim structure.

The high-ohmic (40-200 k Ω) design allows to go in a low-power consumption direction compared with conventional strain gauges. Additionally to the known structures of strain gauges, like pads, supply lines and sensor; structures were integrated to the offset alignment (Figure 11). This is necessary for an efficient bridge signal amplification thus to use the full working range of electronics. The sensor can be trimmed after the gluing on the test item. The influence of the trim on the non-amplified bridge voltage is represented in Figure 12 for two arbitrary sensors (rDMS). After the trim found itself both offset voltages within the range between 0 and about 1 mV.

Manufacturing

A method to process the foils, with high precision in thin film technology and in combination with a lift-off process, was developed for the patterning of the structures. The quality requirements of the used substrates, by structuring with methods of the micro-system technology, are high. In particular, surface roughness and surface ripples should be as low and capable as possible. Additionally, we have adapted all process parameters so that processing regarding adhesion and photolithography on polyimide is possible.

Figure 13 illustrates the process cycle beginning with laminating the foil on the carrier substrate. The high-ohmic resistance sensor structure has a shape like meander and for the temperature compensation was sketched directly as full bridge. The production took place using a lift-off process on 50 μm a thick polyimide foil. The sensor material was sputtered from two sources at the same time and consists of Ni80Cr20 [7]. Depending on the thickness of the layer and the shape of the meanders they were fabricated with different resistances from 30 k Ω to 0.2 M Ω . In order to produce solderable pads and low resistance in the supply lines, the sputtered layer was strengthened with nickel and gold, as represented in Figure 14. Subsequently, all residues of lacquers were removed and the produced foil was replaced from the carrier substrate. In the following step, all sensors were annealed at 200 $^{\circ}\text{C}$ for 20 hours in air and separated thereafter.

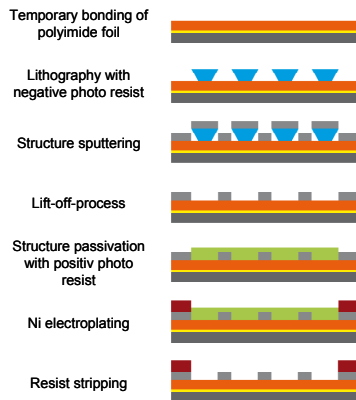


Figure 13. Process flow for the high-ohmic resistive strain gauges.

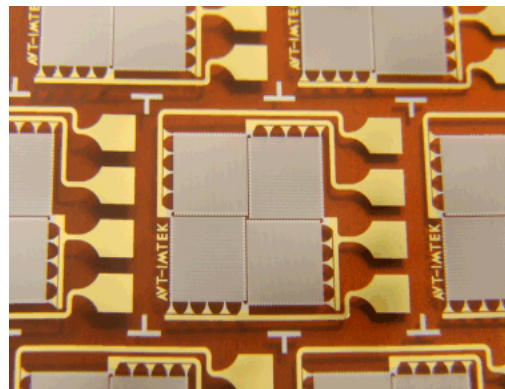


Figure 14. Resistive strain gauges as full bridge.

Characterisation

During the investigation of the resistive strain gauges, we observed a very linear dependence between voltage and strain (Figure 15). As a test specimen for the high-ohmic resistance strain gauges, the mentioned steel ribbon was selected. For characterisation, the sensor prototypes were mounted with an acrylic adhesive on the steel ribbon. The tensile testing set up was also integrated into a heat chamber. So it was possible to measure the influence of temperature on the sensor signal. The difference in the output signal between 25 $^{\circ}\text{C}$ and 85 $^{\circ}\text{C}$ is shown in Figure 15.

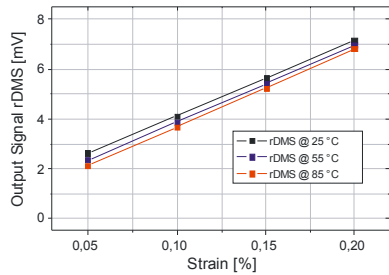


Figure 15. Influence of temperature on output signal.

Table 1. Comparison with usual strain gauges.

	commercial strain gauges (0 ... 1 k Ω)	high-ohmic strain gauges (30 ... 200 k Ω)
Power Electronic	< 1 mW	< 1 mW
Power Sensor	> 4 mW	< 0,13 mW
Total Power	5 mW	1,1 mW

The influence of the temperature can be handled as a static off-set and is correctable with an additional temperature sensor. During the investigation of power consumption of the high-resistance strain gauges, we observed that the power consumption of the system is five times lower in comparison with usual strain gauges, as shown in Table 1. This value can be essentially amplified by appropriate choice and programming of the microcontroller.

COMPARISON CAPACITIVE STRAIN GAUGES WITH RESISTIVE STRAIN GAUGES

Both sensors types, capacitive and high-resistance (40 k Ω), were made and qualified. These strain gauges were mounted on test structures made of steel and characterised experimentally. Their sensitivities as well as their cross-sensitivities to temperature and humidity were analysed. The verified gauge factors of both sensor principles were very similar to the ones, known for conventional strain gauges.

Table 2. Properties of the resistive and capacitive strain gauges.

Principle	Signal Variation	Sensor Properties	Operation Range
		k-Factor	Strain
Capacitive	0.42 %	1.4	0...0.3 %
Resistive	0.63 %	2.1	
		TCR [ppm/K]	Temperature
Capacitive	23 %	2168	-20...85 °C
Resistive	2.2 %	206	
		HCR [ppm/%rLF]	Humidity
Capacitive	0.53 %	55	0...100 % rLF
Resistive	0 %	-	

Although the capacitive strain gauges clearly need less energy (68%) than high-resistance strain gauges, the disadvantage of the higher temperature cross-sensitivity is too significant. Table 2 shows the main properties of the resistive strain gauges made on polyimide and the capacitive strain gauges made on LCP.

RDMS DEMONSTRATOR

For the realisation of energy-efficient strain gauges demonstrator, it was necessary to find suitable circuits with very low energy consumption. The output signal from the strain gauges must be digitised before the signal can be processed and can be wireless transmitted (Figure 16). The resistive strain gauges output signal is given as voltage

change between 0 and 7 mV at an operating voltage of 6 Volt and a strain of 1 %. The selected energy-saving microcontroller with integrated radio module (CC430, by Texas Instruments) expects the signals with voltages between 0 and 1.5 V. Therefore the output signals must be amplified with an energy-saving amplifier to this level. At present the best economical zero drift instrumentation amplifier is the INA333 (by Texas Instruments) with a standby current of 75 μ A. The standby current from the microcontroller amounts 1 μ A.

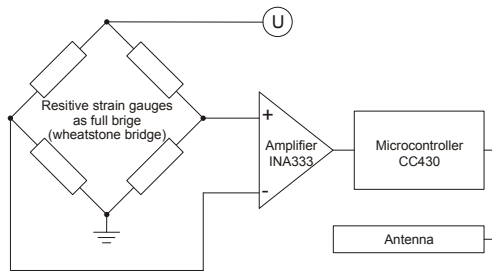


Figure 16. Block diagram for rDMS demonstrator.

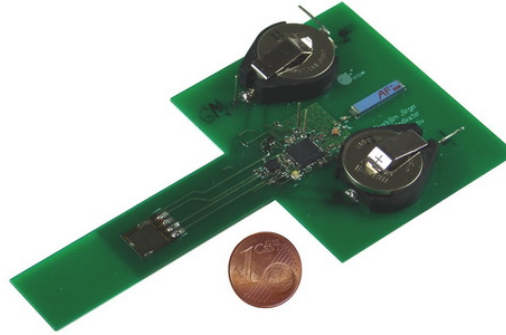


Figure 17. rDMS demonstrator.

We found out, that the settling time of electronics is so small, so that the complete electronics can run in sleep modus and will be waked up only for the actual measurements. The radio module has the highest energy consumption from all components of the microcontroller. As the radio module has an own sleep modus, the sampling frequency of strain gauges can be independent from the wireless data communication.

The purpose of condition monitoring is to record the variations over the time. The memory capacity of the microcontroller amounts 32 kByte. This is enough space to save the raw data for the condition monitoring depending on the sampling rate. So data transfer is only rarely necessary. In many cases only the data distribution is needed as information. A histogram representing load collectives needs substantially less memory than the time series of the raw data. In practice the condition monitoring is independent from the sampling rate and also independent from the data transfer frequency. The shown energy-efficient resistive strain gauges demonstrator (rDMS) works with these reported components (Figure 17).

CONCLUSION

Our conclusion based on this work is, that the proven strain gauge concept has been developed further towards intelligent and monitoring strain gauges, as low-loss capacitive and resistive strain gauges were made available. It was verified that the energy consumption of the demonstrated condition monitoring circuits is reduced approximately by a factor of five, as a result of the novel transducer structures.

References

1. Wang & Gao, "Condition Monitoring and Control for Intelligent Manufacturing", Springer, Berlin, 2006.

2. Matsuzaki: „Wireless flexible capacitive sensor based on ultra-flexible epoxy resin for strain measurement of automobile tires“, Sensors and Actuators, A 140 S 32-42, 2007.
3. Aebersold, “Design, modelling, fabrication and testing of a MEMS capacitive bending strain sensor”, Computers and Typesetting, Vol. 34 Addison-Wesley, 2006.
4. Igreja, Dias, “Analytical evaluation of the interdigital electrodes capacitance for a multi-layered structure”, Sensors and Actuators, A 112 S. 291-301, 2004.
5. Melcher, “Dielectric effects of moisture in polyimide”, IEEE Transactions on Electrical Insulation, Vol. 24 S. 31–38, 1989.
6. Zhang Xia, “Development of SOP module technology based on LCP substrate for high frequency electronics applications”, Electronics Systemintegration Technology Conference, S. 118–125, 2006.
7. Petrovic, Bundaleski, Radovic et al.: “Structure and surface composition of NiCr sputtered thin films”, Science of Sintering, 38:155–160, 2006.